Review

Israel Journal of Chemistry

DOI: 10.1002/ijch.201400112

Issues and Challenges for Bulk-Type All-Solid-State Rechargeable Lithium Batteries using Sulfide Solid Electrolytes

Yoon Seok Jung,*[a] Dae Yang Oh,[a] Young Jin Nam,[a] and Kern Ho Park[b]

Abstract: As lithium rechargeable batteries are considered a potential candidate for large-scale energy storage applications in devices such as electric vehicles (EVs) and smart grids, their safety has become of prime concern. This calls for the need to replace the flammable organic liquid electrolyte (LE) with an inorganic solid electrolyte (SE), and thus, develop bulk-type all-solid-state lithium batteries (ASLBs), fabricated using a scalable process. Sulfide SEs are considered the most competitive candidate owing to their high conductivity at room temperature (10^{-3}–10^{-2} S cm^{-1}), which is comparable to that of LEs, and their ductility, which enables the fabrication of ASLBs simply using cold pressing. In the present review, issues and challenges to be faced for the fabrication of bulk-type ASLBs using sulfide SEs are presented and discussed, with a special focus on the development of SEs, compatibility of the electrode materials with SEs, and structure of the composite electrodes. Recent progress made with the aim of addressing the aforementioned issues and challenges is also presented, to provide an outlook on the future of SEs and ASLBs.

Keywords: batteries · conducting materials · lithium · solid electrolyte · sulfides

1. Introduction

Since Sony Corporation commercialized the first products featuring lithium-ion batteries (LIBs) in the early 1990s,[1] LIBs have begun to emerge as the most suitable power source for portable electronic devices.[2] The most important advantage of LIBs is their high energy density, which originates from their high voltage of ~4 V.[2] Since the electrochemical window typical of aqueous liquid electrolytes (LEs) impedes LIBs reaching such a high voltage, the development of organic LEs was the basis of the success of the LIB.[2] The state-of-the-art organic LEs consist of a lithium salt, such as $LiPF_6$, dissolved in a mixture of linear and cyclic alkyl carbonates, exhibiting an ionic conductivity of ~10^{-2} S cm^{-1} at room temperature (RT).[2a,d] However, the intrinsic nature of organic LEs poses serious safety concerns regarding their flammability and possible leakages.[2,3] The safety of LIBs is of prime concern because they are considered a potential candidate for large-scale energy storage applications in devices such as electric vehicles (EVs) and energy storage systems.[2–4] All-solid-state lithium batteries (ASLBs) using inorganic solid electrolytes (SE) are considered as an ideal alternative to ultimately realize safe LIBs.[3a,4] Their broad operating temperature range is also an important benefit from the point of view of energy storage applications.[3c,5] Additionally, SEs offer two significant advantages over LEs. First, only the cation, Li^+, is mobile; thus, its transport number is 1. Second, Li^+ ions at the electrode/SE interface are not subject to desolvation, with positive effects on the charge transport, which explains the appreciable amount of activation energy and the related kinetic properties typical of LE cells.[2d,6] Considering these two features, it is reasonable that batteries using SEs may outperform batteries using LEs, if the ionic conductivity is the same.[6b]

Thin film ASLBs using LiPON ($Li_{3.3}PO_{3.9}N_{0.17}$) as the SE are well-known commercialized batteries showing excellent performance.[7] However, the use of thin film ASLBs is restricted to small-scale applications, such as smart cards and microelectronic devices, due to the highly expensive vacuum deposition process required for their fabrication.[7,8] Recently, great attention has been paid to

[a] Y. S. Jung, D. Y. Oh, Y. J. Nam
School of Energy and Chemical Engineering
Ulsan National Institute of Science and Technology (UNIST)
50 UNIST-gil, Ulju-gun
Ulsan 689-798 (South Korea)
Tel.: (+82) 52-217-2944
Fax: (+82) 52-217-3009
e-mail: ysjung@unist.ac.kr

[b] K. H. Park
School of Chemical and Biological Engineering
Seoul National University
599 Gwanangno, Gwanak-gu
Seoul 151-742 (South Korea)

Israel Journal of Chemistry

a bulk-type (or composite-type) ASLB suitable not only for portable electronic devices, but also for large-scale applications.[3a,4,9] As shown in Figure 1, a critical feature of

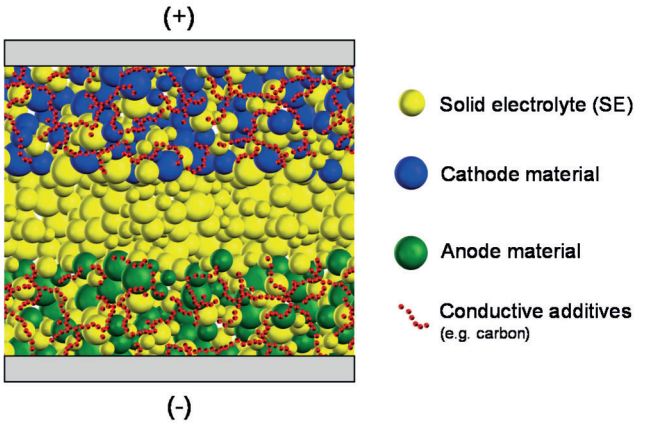

Figure 1. Schematic diagram of bulk-type all-solid-state lithium batteries (ASLBs) using sulfide solid electrolyte (SE).

the bulk-type ASLB is its composite electrode structure, in which the active materials, SE powders, and the conductive materials, such as carbon, exist as particulate mixtures. Bulk-type ASLBs do not need any expensive vacuum deposition process to be fabricated, which is promising for large-scale applications. In the bulk-type ASLBs, SE particles replace the LE typical of conventional LIBs. The thick composite-structured electrode in the bulk-type ASLBs is an indication their energy density can be increased, thus making them compete with conventional LIBs. However, this requires highly conductive SEs which exhibit ionic conductivity comparable to that of LEs (~10^{-2} S cm^{-1} at RT).

To date, many SEs with conductivities over 10^{-4}–10^{-3} S cm^{-1} at RT have been developed, as seen in Figure 2.[3a,4,10] Among the materials suitable to be used as SEs, oxides[10f–h] and sulfides[3a,4,10a–d] have been extensively investigated for ASLBs.

Yoon Seok Jung is a Professor in the School of Energy and Chemical Engineering at UNIST, Korea. He received his BS degree (2001) and Ph.D. (2008) in Chemical Engineering from Seoul National University, Korea. Before he joined UNIST in 2011, he worked as a postdoc fellow at the University of Colorado in Boulder (2008–2009), at the University of Texas at Austin (2009), and at the National Renewable Energy Laboratory (2009–2011), USA. His current research is focused on electrode materials and solid electrolytes for rechargeable batteries.

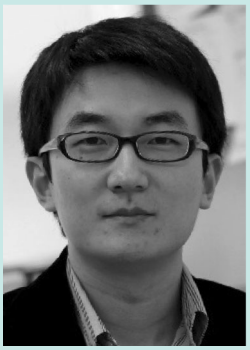

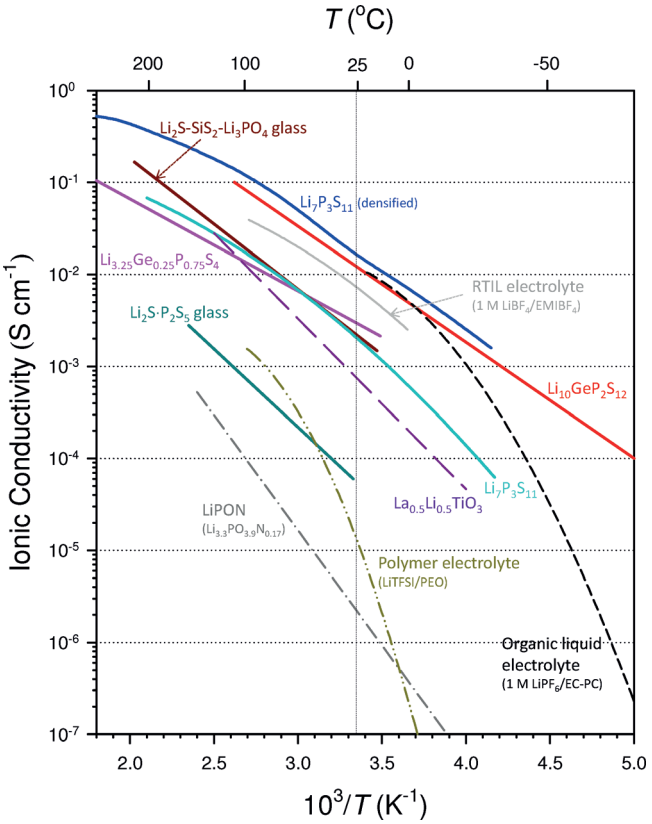

Figure 2. Ionic conductivity of various sulfides suitable for SEs as a function of temperature. The ionic conductivities of other liquid and solid electrolytes (LEs and SEs) are shown for comparison.[3a,4]

The perovskite-structured $Li_{3x}La_{2/3-2x}\square_{1/3-2x}TiO_3$ ($0<x<0.16$) (LLT),[10f] the NASICON-structured $Li_{1.3}Al_{0.3}Ti_{1.7}(PO_4)_3$,[10g] and the garnet-structured $Li_7La_3Zr_2O_{12}$ (LLZ)[10h] are the most famous oxides used as SE materials. They exhibit conductivities in the range of 10^{-4}–10^{-3} S cm^{-1} at RT, which is acceptable for bulk-type ASLBs, although not ideal. They can be handled in an atmospheric environment, which is another advantage. However, their brittleness poses a critical restriction for the fabrication of bulk-type ASLBs.[9,11] Cold pressing of a mixture of active materials with a selected oxide as the SE is not enough to form the favorable two-dimensional contacts necessary for an effective Li^+ ionic conduction throughout the three-dimensional composite electrode structure.[9,11] Instead, a sintering process at elevated temperature is necessary.[11] This kind of heat treatment generates unwanted interfacial reactions, resulting in the failure of bulk-type ASLBs using one of these oxides as the SE during operation.[11] However, several exceptions exist. ASLBs with the phosphate-based material, $Li_3V_2(PO_4)_3$, used as the electrode, and the phosphate-based material, $Li_{1.5}Al_{0.5}Ge_{1.5}(PO_4)_3$, used as the SE by sintering via the spark plasma method, gave a performance of ~100 mA h (g of $Li_3V_2(PO_4)_3)^{-1}$.[12] The addition of Li_3BO_3 and Al_2O_3 to Ca- and Nb-doped LLZ

could reduce the sintering temperature to 790 °C and the $LiCoO_2$/Li battery could work.[13] However, the cycle test for the $Li_3V_2(PO_4)_3$ ASLB was conducted at a very low C-rate (C/20–C/40) at the temperature of 80 °C.[11] Also, the $LiCoO_2$ ASLB using the Ca- and Nb-doped LLZ sintered with Li_3BO_3 and Al_2O_3 showed a very low discharge capacity of 78 mA h g^{-1} at a very low C-rate (~C/100).[13]

The most important advantage of sulfide SEs over oxide SEs is that the former can be easily deformed, simply by cold pressing.[3b,9] The research group of Tatsumisago reported that $Li_2S{\cdot}P_2S_5$ SE materials display Young's moduli between the one typical of oxide ceramics and the one typical of organic polymers.[9] The unwanted interfacial reaction between the electrode materials and the SEs occurring during the fabrication process, may consequently be avoided. This encourages a more extensive investigation on sulfide SEs for ASLBs.[3a,5,14]

In the following sections, we will discuss the issues and challenges when using sulfide SEs for bulk-type ASLBs, from the development of SEs, in terms of improving their ionic conductivity, stability in air, and electrochemical stability, to their compatibility with the electrode materials, particularly when using lithium metal as the anode, Li_xMO_2 (M = Co, Ni, Mn), and sulfur or Li_2S as the cathode, but also considering innovative electrode materials. Finally, we will describe and discuss the design of composite electrodes.

2. Conductivity of Solid Electrolytes

The high ionic conductivity of SEs, compared with that of LEs (~10^{-2} S cm^{-1}), is the prerequisite for the employment of high-energy ASLBs at ambient temperature. The main constraints on the material design of SEs can be summarized as follows. First, the larger and the more polarizable the ions, the more preferable they are for achieving higher ionic conductivity.[10a,15] It is known as a general trend that the isovalent substitution of oxygen with the larger and more polarizable sulfur tends to increase the conductivity of the compound.[10a] Second, the creation of an interfacial vacancy caused by the aliovalent substitution can strongly affect the ionic conductivity.[10a] In 2001, Kanno and co-workers reported the thio-lithium superionic conductor (thio-LISICON, $Li_{3.25}Ge_{0.25}P_{0.75}S_4$), which was the first crystalline ionic conductor having a high ionic conductivity (2.2×10^{-3} S cm^{-1} at 25 °C) and a high decomposition potential.[10a] Recently, the same group published a work on $Li_{10}GeP_2S_{12}$ (LGPS, 1.2×10^{-2} S cm^{-1} at RT).[3a] Even though thio-LISICON and LGPS do not present an identical structure, both are based on the concept of aliovalent substitution: both have the same chemical formula, $Li_{4-x}Ge_{1-x}P_xS_4$, with $x=3/4$ for thio-LISICON and $x=2/3$ for LGPS. The extremely high conductivity of LGPS triggered an explosion of interest in this field. The *ab initio* calculation of LGPS by Ceder and co-workers claimed ionic conductivities of 4×10^{-2} S cm^{-1} in the *c*-direction and 9×10^{-4} S cm^{-1} in the *ab* plane.[16] The calculated overall conductivity[16] of 9×10^{-3} S cm^{-1} agrees well with the experimental value (1.2×10^{-2} S cm^{-1}).[3a] This result suggests that the ionic conduction in LGPS occurs in three dimensions, rather than in one dimension. The isotropy of ionic conduction in LGPS was also confirmed by the structure investigation performed using single-crystal X-ray analysis.[17] The theoretical approach for the $Li_{10\pm1}MP_2X_{12}$ family (where M = Ge, Si, Sn, Al, or P, and X = O, S, or Se) anticipated that the isovalent substitution of germanium into cheaper elements, including silicon or tin, would have small effects on the ionic conductivity of the compound.[18] The high conductivity of 4×10^{-3} S cm^{-1} at 27 °C, obtained experimentally using $Li_{10}SnP_2S_{12}$, is in line with the aforementioned theoretical calculations.[19] The aliovalent substitution of tin with arsenic in Li_4SnS_4[20] to give $Li_{4-x}Sn_{1-x}As_xS_4$, where $x=0.125$, was also demonstrated to significantly increase the conductivity of the compound from 7.1×10^{-5} S cm^{-1} to 1.39×10^{-3} S cm^{-1} at 25 °C.[10d]

$Li_2S{\cdot}P_2S_5$ glass-ceramics are another important class among the sulfides used for SEs. Crystallization of $Li_2S{\cdot}P_2S_5$ glassy powders at elevated temperatures improved the conductivities of the obtained compounds, giving values of ~10^{-3} S cm^{-1}.[10b,21] The glass-ceramic powders were obtained by the heat treatment of glassy powders prepared from mechanical milling or melt-quenching methods.[10b,21a–e] The compound $xLi_2S{\cdot}(100-x)P_2S_5$ with $x=70.0$–80.0 has been extensively studied.[10b,21a–e] Particularly, stoichiometric $Li_7P_3S_{11}$ (or $70Li_2S{\cdot}30P_2S_5$) and $Li_7P_3S_{11-z}$ exhibited the highest conductivities at 25 °C: 4.2×10^{-3} S cm^{-1} and 5.4×10^{-3} S cm^{-1}, respectively.[21e,f] It should be noted that the contribution to the resistance given by the grain boundaries becomes more important for highly conductive materials. Recently, the conductivity of $Li_7P_3S_{11}$ was measured after optimizing the heat treatment of the SE pellet, so that the grain boundary resistance could be minimized by densification, allowing the conductivity to reach 1.7×10^{-2} S cm^{-1} at RT, a value even higher than that of LGPS (1.2×10^{-2} S cm^{-1}).[4] Glass-ceramic SEs doped by germanium were also studied.[22] Advantages of the glass-ceramic SEs over the crystalline ones might include their relatively lower heat-treatment temperature. Crystallization of glassy sulfides occurs at ~200–300 °C, which is, in turn, the temperature for preparation of the glass-ceramic SEs.[10b,21] In contrast, the crystalline SEs are prepared at ~450–600 °C[3a,10a,d,19,23]. Another family of crystalline sulfides used as SEs, Li-argyrodite Li_6PS_5X (X = Cl, Br, I), also exhibited a high conductivity of 10^{-4}–10^{-3} S cm^{-1} at 25 °C.[23] Table 1 summarizes the ionic conductivities of various crystalline and glass-ceramic SEs.

Glassy sulfides were studied extensively before the crystalline (e.g., thio-LISICON and LGPS) and glass-ceramic materials were reported. Glassy sulfides for SEs in-

Table 1. Ionic conductivity of crystalline and glass-ceramic sulfide SEs.

Composition	Structure	Conductivity ($\times 10^{-3}$ S cm^{-1})	Activation energy (kJ mol^{-1})	Reference
$Li_{3.25}Ge_{0.25}P_{0.75}S_4$ (Thio-LISICON)	Crystal	2.1[a]	20	[10a]
$Li_{10}GeP_2S_{12}$	Crystal	12[a]	24	[3a]
Li_6PS_5Cl (Li-argyrodite)	Crystal	1.33	29–39	[23b]
$Li_{3.833}Sn_{0.833}As_{0.166}S_4$	Crystal	1.39	20	[10d]
$Li_{10}SnP_2S_{12}$	Crystal	4		[19]
$Li_7P_3S_{11}$	Glass-ceramic	1.4[b]/4.2[c]/5.4[d]/17[a]	17[a]	[4, 21e]

[a] Measured using the pellet densified at elevated temperature. [b] Measured using the cold pressed pellet (Ref. 4). [c] Measured using the cold pressed pellet (Ref. 21e). [d] $Li_7P_3S_{11-z}$. Measured using the cold pressed pellet (Ref. 21e).

clude $Li_2S{\cdot}P_2S_5$,[24] $Li_2S{\cdot}SiS_2{\cdot}Li_3N$,[25] $Li_2S{\cdot}P_2S_5{\cdot}LiI$,[26] $Li_2S{\cdot}SiS_2{\cdot}LiI$,[27] $Li_2S{\cdot}SiS_2{\cdot}Li_xMO_y$,[28] $Li_2S{\cdot}GeS_2$,[29] and $Li_2S{\cdot}B_2S_3{\cdot}LiI$,[30] all exhibiting conductivities in the range of ~10^{-4}–10^{-3} S cm^{-1} at RT.

3. Behavior of Solid Electrolytes in Air

The most serious drawback of sulfide SEs is their chemical instability in air. Sulfide SEs tend to react with the water contained in the air, generating harmful H_2S gases.[10d,31] Among the $Li_2S{\cdot}P_2S_5$ SEs, the ones having an ortho-composition ($75Li_2S{\cdot}25P_2S_5$ or Li_3PS_4) were reported to exhibit the highest stability, reasonably because the PS_4^{3-} ion is more difficult to hydrolyze from the water in the air with respect to other ions, including $P_2S_7^{4-}$.[31] A reduced H_2S generation from sulfide SEs exposed to air was achieved using materials with a new composition. For instance, addition of Li_2O or LiI into $Li_2S{\cdot}P_2S_5$ (to give $7Li_2O{\cdot}68Li_2S{\cdot}25P_2S_5$ and $30LiI{\cdot}70(0.07Li_2O{\cdot}0.68Li_2S{\cdot}0.25P_2S_5)$) significantly decreased H_2S gas generation.[32] Addition of FeS and basic metal oxides, such as CaO, to $Li_2S{\cdot}P_2S_5$ also suppressed the generation of H_2S gas.[33] Interesting results were also achieved using the relatively uncommon Li_4SnS_4[20] as a starting point. Liang and coworkers demonstrated that substituting tin with arsenic in Li_4SnS_4 provided both high ionic conductivity (1.39×10^{-3} S cm^{-1} at RT) and outstanding chemical stability to water.[10d] Figure 3 shows that the changes in the structure and ionic conductivity of $Li_{3.833}Sn_{0.833}As_{0.166}S_4$ SEs after exposure to humid air were negligible.[10d] The excellent chemical stability of $Li_{4-x}Sn_{4-x}As_xS_4$ can be explained by the theory that soft acids, such as tin and arsenic, preferentially react with soft bases, like sulfur, rather than with hard acids, like oxygen.[10d]

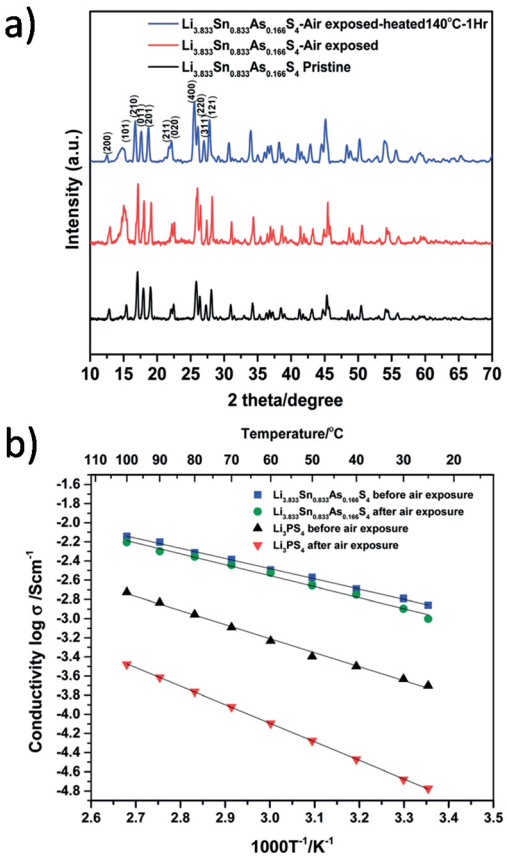

Figure 3. a) XRD patterns and b) Arrhenius plots for a $Li_{3.833}Sn_{0.833}As_{0.166}S_4$-based SE before and after air exposure. Results of β-Li_3PS_4 are shown for comparison. Adapted with permission from Ref. [10d].

4. Electrochemical Stability of Solid Electrolytes

It is well known that the electrochemical stability of LEs plays a main role in the performance, such as durability, rate capability, and safety, of the LIBs.[2,34] The importance of the electrolyte electrochemical stability is high, and is therefore also desired in the case of SEs. For example, even though Li_3N exhibits a high ionic conductivity of 10^{-3} S cm^{-1}, its low decomposition potential of ~0.4 V (vs. Li/Li$^+$) impedes its employment in ASLBs.[3c] Another example is given by the oxide SEs. The perovskite-structured LLT undergoes decomposition in contact with metallic lithium because Ti^{4+} cations are reduced to Ti^{3+}.[10f]

However, the invention of LLZ, with fixed-valent zirconium in place of the titanium, solved this problem.[10h]

Although it is not yet well known, sulfide SEs also have limited electrochemical windows. Theoretical calculations carried out for the $Li_{10\pm1}MP_2X_{12}$ family (where M = Ge, Si, Sn, Al, or P, and X = O, S, or Se) provide an insight on the electrochemical stability of various materials used for SEs.[18] The band gap of LGPS was calculated to be 3.6 eV, suggesting a relatively narrow electrochemical window.[18] Germanium in LGPS is believed to be reduced at a low potential,[35] similar to titanium in LLT.[10f] Li_2S and P_2S_5 are expected to be formed as a result of decomposition.[18] Recently, Jung and co-workers confirmed that the structure of LGPS is altered even at 0.6 V (vs. Li/Li^+), most likely forming an Li_2S phase, which explains the significant degradation in the performance of TiS_2/LGPS/Li-In solid-state batteries.[35] The $Li_2S{\cdot}P_2S_5$-based SEs turned out to be more stable at low voltages than the LGPS-based SEs, as shown in Figure 4. At positive voltage ranges, the onset voltage triggering the oxidative decomposition is ~3.0 V (vs. Li/Li^+).[14e,36]

Even though the restricted electrochemical stability can degrade the performance of ASLBs, the electrochemical window itself does not directly limit the operating voltage range of ASLBs. Graphite has been successfully employed in LIBs, in spite of the decomposition of LEs occurring at <1 V (vs. Li/Li^+).[2a] In addition to the intrinsic electrochemical stability of the electrolyte, a favorable passivation is important, because it may suppress the continuous process of decomposition.[2a] In this context, the engineering of the interface between the active material and the SE is a critical issue in ASLBs, and this will be discussed in the following section.

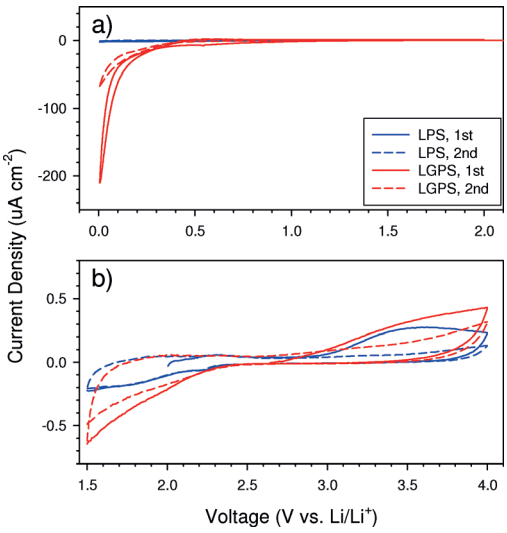

Figure 4. Cyclic voltammograms of Ti/Li_3PS_4 (LPS)/LiIn and Ti/LGPS/LiIn cells: a) in the negative potential range; and b) in the positive potential range. Adapted with permission from Ref. [35].

5. Compatibility of Electrode Materials with Solid Electrolytes

The success of state-of-the-art LIBs may be attributed not only to the use of suitable electrode materials, but also to the carbonate-based LEs, with their kinetically wide electrochemical windows and their excellent compatibility with the electrode materials.[2] For example, fully reversible intercalation-deintercalation in $LiVS_2$ became possible when using the electrolyte which is commonly used nowadays, namely 1 M $LiPF_6$ in ethyl carbonate:diethyl carbonate (1:1 vol. ratio), whereas the traditional electrolyte used for the studies performed in the 1970s, 1 M $LiClO_4$ in propylene carbonate, had a detrimental effect on the performance of $LiVS_2$.[37] Understanding the phenomena taking place at the interface between the sulfide SEs and the electrode materials is crucial. In addition, new opportunities may arise to (re)investigate the compatibility of already known or innovative electrode materials with the sulfide SEs.

5.1. Lithium Metal

Lithium metal is supposed to be an ideal anode for all types of lithium secondary batteries, including alternative batteries such as Li-S and Li-air batteries, because of its high theoretical capacity (3862 mA h g^{-1}), the lowest operating potential among all the known anode materials, its metallic nature, and the fact that it avoids the use of prelithiated cathode materials.[38] However, a severe safety concern, associated with eventual internal short circuits caused by the dendritic growth of lithium during repeated deposition and dissolution cycles, brought the ban of lithium metal in commercially available LIBs.[39] The ASLB, which is free from flammable components, can take advantage of the use of lithium metal as the anode, maximizing its energy density.

Two issues, however, must be addressed. First, ASLBs also suffer from the internal short circuits caused by abnormal lithium growth. In the experiments carried out using the $Li_2S{\cdot}P_2S_5$ SE pellet shown in Figure 5a and Figure 5b, it was observed that lithium metal tends to grow in the voids and along the grain boundaries of the SE pellet.[40] As a result, a sign of internal short circuit in the charge voltage profile (indicated by the arrow) is usually observed, as shown in Figure 5c. It was observed that during charging (or delithiation) of $LiTiS_2$, metallic lithium was deposited on the Li metal anode, leading to the growth of lithium in the voids and along the grain boundaries of the cold pressed SE layer. Second, the chemical stability of the SEs in contact with lithium metal can be affected by its composition. Jung and co-workers reported that the structure of LGPS is severely altered at low voltage ranges, likely generating a Li_2S phase.[35] The poor chemical stability of the SE in contact with lithium was also found in the As-doped Li_4SnS_4, in which tin acts as

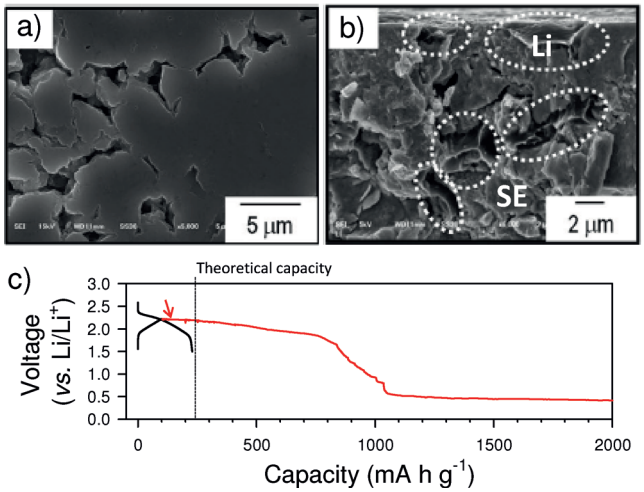

Figure 5. SEM images of a) $80Li_2S{\cdot}20P_2S_5$ SE surface before cycling; and b) $80Li_2S{\cdot}20P_2S_5$ SE cross-section after lithium deposition on the side of a stainless steel (SS) current collector in all-solid-state cells of Li/SE/SS. Adapted with permission from Ref. [40]. c) First discharge-charge voltage profile of TiS_2/SE/Li cell at 0.075 mA cm^{-2} at 30°, with the $75Li_2S{\cdot}25P_2S_5$ glass-ceramic as the SE.

a reducing center.[10d] A protective coating on $Li_{3.833}Sn_{0.833}As_{0.166}S_4$, made with $3LiBH_4{\cdot}LiI$, enabled the reversible cycling of lithium metal.[10d] A thin indium layer prepared by vacuum evaporation can be employed to achieve good cyclability of $Li/Li_4Ti_5O_{12}$ cells at high current density, due to the intimate contacts formed at the SE/Li interface.[41] Enabling the use of lithium metal as the anode will remain a challenge until significant developments of composition, surface modifications, and pelletized microstructure of SEs are made.

5.2. Li_xMO_2

As for the conventional LIBs using LEs, the layered or spinel Li_xMO_2 (M = Co, Ni, Mn) cathode materials are considered as viable candidates for ASLBs because of their highly reversible intercalation-deintercalation reaction with low dimensional change and high operating potential. To date, many Li_xMO_2 materials, including $LiCoO_2$,[3a,5a,9,14d,23b,c,32,36,41,42] $Li[Ni,Mn,Co]O_2$,[42ae,43] and $LiMn_2O_4$,[42aa] have been tested in ASLBs using sulfide SEs. However, the bare Li_xMO_2 showed much lower capacity than the theoretical one, a large amount of irreversible reaction during charging, and a high overpotential, shown in Figure 6.[42h] The poor performance of Li_xMO_2 originate from the intrinsically low oxidation onset potential (~3 V vs. Li/Li$^+$) of the sulfide SEs,[14e,36] as confirmed by the abnormal sloping plateau starting at ~2.3–2.4 V (vs. LiIn), shown in Figure 6a.[42h] Tatsumisago and co-workers investigated the interface between $LiCoO_2$ and $Li_2S{\cdot}P_2S_5$ SE after charging using electron microscopy.[5a] It was observed that the elements originally found in $LiCoO_2$ and $Li_2S{\cdot}P_2S_5$ SE mutually diffuse, as shown in Figure 7.[5a]

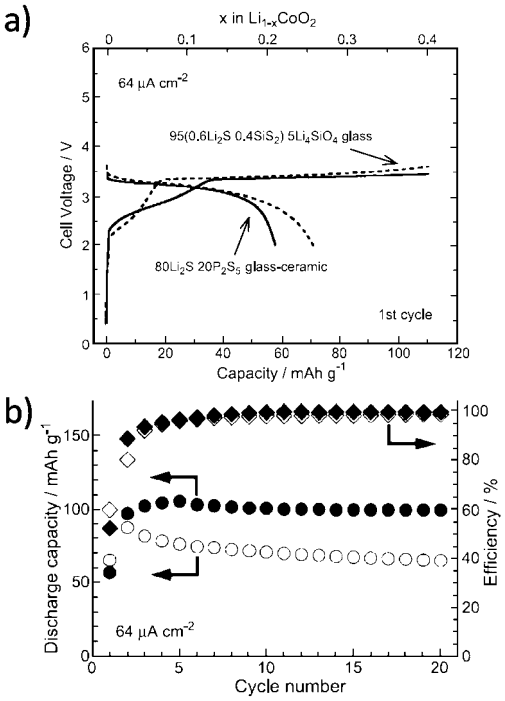

Figure 6. a) First charge and discharge voltage profiles; and b) cycle performance for $LiCoO_2$/SE/In cells. Adapted with permission from Ref. [42h].

The formation of a new interfacial layer, mainly consisting of cobalt and sulfur, was suggested to be the cause of the poor performance.[5a] Takada and co-workers adopted the "space-charge layer theory"[44] to explain the poor behavior at the interface between $LiCoO_2$ and the sulfide SE.[14d,42n,aa,ab,45] Depletion of lithium in the sulfide SE near the Li_xMO_2 accounts for the huge interfacial resistance, and is reasonably caused by the diffusion of lithium triggered by the large difference in chemical potentials between Li_xMO_2 and the sulfide materials.[14d,42n,aa,ab,45]

As already reported by numerous publications regarding oxide cathodes for LIBs containing LEs,[34,46] surface coatings made using various metal oxides, such as $LiNbO_3$,[3a,42n] $Li_4Ti_5O_{12}$,[14d] Li_2SiO_3,[36a] Al_2O_3,[42x] and $BaTiO_3$,[45b] when applied on Li_xMO_2, turned out to be effective for significantly reducing the interfacial resistance in ASLBs, thereby improving their electrochemical performance, as shown in Figure 8.[5a] The mechanism underlying the observed enhancement can be either the suppression of chemical reactions between the sulfide and the oxide layers, or the shielding effect provided by the oxide coatings against the noble potential of the Li_xMO_2 cathodes.[14d,42n,aa,ab,45] It should be emphasized that typically, the coatings with electron-insulating and ion-conducting oxide materials resulted in improvement of performance.[14d,42n,aa,ab,45] Enhanced performance of $LiCoO_2$ by electronically conductive coatings with metal sulphides, such as NiS and CoS, were also reported.[42z] Ion conductivity can be achieved by using coating materials that

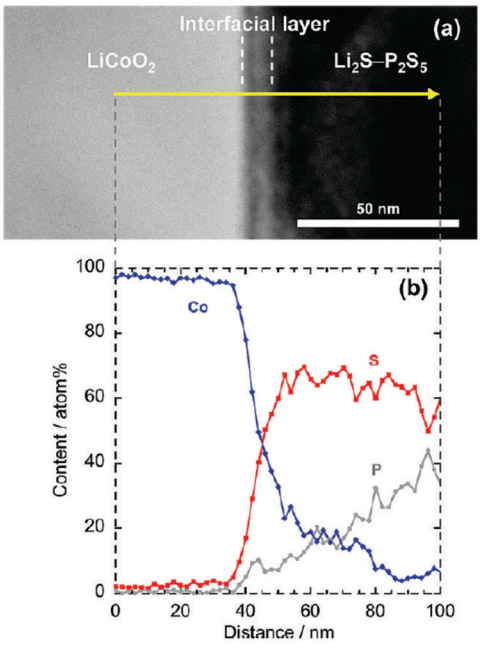

Figure 7. a) Cross-sectional high-angle annular dark field scanning transmission electron microscopy (HAADF-STEM) image of $LiCoO_2$/$Li_2S{\cdot}P_2S_5$ interface after initial charging; and b) cross-sectional energy dispersive X-ray spectroscopy (EDX) elemental line profiles. Adapted with permission from Ref. [5a].

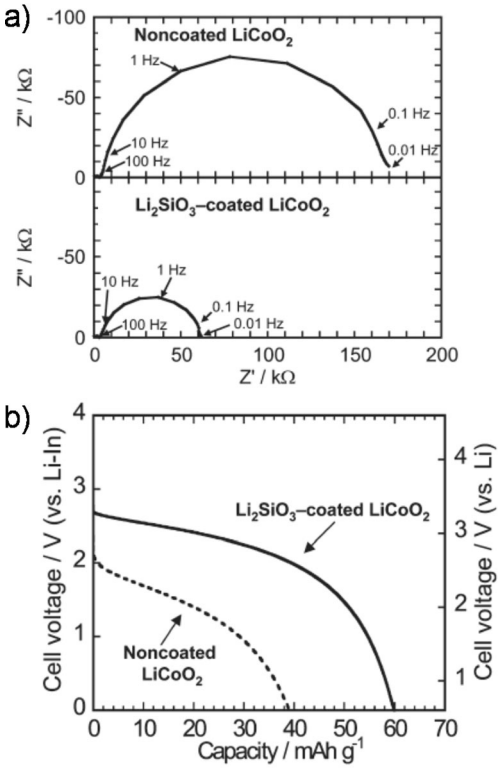

Figure 8. Comparative a) Nyquist plots; and b) discharge voltage profiles, of the bare and Li_2SiO_3-coated $LiCoO_2$/$Li_2S{\cdot}P_2S_5$/In cells at −30 °C. Adapted with permission from Ref. [5a].

include lithium.[3a,14d,36a,42n] However, a good ion conductivity was also found in a lithium-free tantalum oxide, in which openings in the crystal structure were large enough for Li^+ ions to pass through.[47] The majority of conventional coatings were applied using wet-chemical methods.[3a,14d,36a,42n,46c] Recently, however, it has been reported that coatings applied via atomic layer deposition (ALD) on various electrode materials enhanced the performance and safety of LIBs containing LEs.[34,46d,e,48] Since ALD is based on a sequential and self-limiting surface reaction, ultra-thin coatings, with a thickness lower than 1 nm, can be obtained, with an accuracy of one atomic layer.[49] Al_2O_3 was also applied via ALD to $LiCoO_2$ ASLBs, significantly improving their performance.[42x]

5.3. Sulfur and Li_2S

Elemental sulfur is a promising cathode material for rechargeable lithium batteries, due to its theoretically extremely high capacity ($S+2Li^+ +2e^- \leftrightarrow Li_2S$, 1672 mA h (g of S)$^{-1}$ or 1167 mA h (g of Li_2S)$^{-1}$).[38b] Although the low operating voltage (~2.1 V vs. Li/Li^+) is disadvantageous for the energy density, it avoids any noticeable decomposition of the sulfide SE.[35,36] Moreover, the problem of the dissolution of polysulfide intermediate products, encountered in the LE-based LIBs, and leading to an extremely poor coulombic efficiency, is not a concern for the ASLBs.[14a,38b] Therefore, sulfur and lithiated sulfur, Li_2S, are regarded as ideal cathode materials for achieving a high energy density in ASLBs. However, the electrical insulation properties[14a,38b] and the massive volume change during charge and discharge (~179 %)[14e,f] remain obstacles to be overcome for the eventual success of sulfur-based ASLBs.

The formation of a nanocomposite structure from the combination of sulfur or Li_2S with carbon is the most versatile strategy to improve the performance of ASLBs.[14a,50] The size of sulfur or Li_2S particles is critical, not only to relieve the stresses induced by the volume changes during charge and discharge, but also to maximize the extension of the electrically active domains. Carbon can provide conduction pathways for the insulating sulfur or Li_2S, and at the same time, can act as a buffering phase for the volume change. Nanostructured sulfur-carbon or Li_2S-carbon materials for ASLBs were prepared by ball-milling (BM)[14a,50b,d–f] and gas-phase mixing (or melt diffusion mixing).[50a,c] Table 2 summarizes the performance of various sulfur-based and Li_2S-based cathode materials for ASLBs. Notably, the intimate ionic contacts achieved by BM between the sulfur-carbon or Li_2S-carbon and the SE are critical for the enhancement of the capacity and rate capability, as shown in Figure 9.[14a,50b,d–f] For example, the BM of a mixture of sulfur, activated carbon, and amorphous $Li_{1.5}PS_{3.3}$ resulted in a capacity of ~1600 mA h (g of S)$^{-1}$, which is close to the theoretical capacity.[44e] The phosphorus/sulfur ratio was

Table 2. Electrochemical performance of sulfur and Li_2S electrode in ASLB.

Sample	Preparation method	Reversible capacity (mA h (g of Li_2S or S)$^{-1}$/mA h (g of electrode)$^{-1}$)	Current density (mA cm^{-2})	Composition of electrode[f]	SE	Voltage range (V vs. Li/Li$^+$)	Loading of electrode (mg cm^{-2})	Reference
S-Cu	BM	867/245	0.064	S-Cu : AB : SE = 20 : 3 : 30[d]	$80Li_2S \cdot 20P_2S_5$	0.85–3.35	12.7	[51a]
Li_2S-Cu	BM	653/186	0.064	Li_2S-Cu : AB : SE = 38 : 5 : 57[d]	$80Li_2S \cdot 20P_2S_5$	0.6–3.6	12.7	[51c]
S-carbon	BM	1550/388 1100/275	0.064 1.3	S : AB : SE = 25 : 25 : 50	$80Li_2S \cdot 20P_2S_5$	1.6–2.6 1.3–3.3	12.7	[50b]
Li_2S-carbon-SE	BM	800/200 580/145	0.064 1.3	Li_2S : AB : SE = 25 : 25 : 50	$80Li_2S \cdot 20P_2S_5$	0.6–3.6	12.7	[14a]
S-carbon-SE	BM	1200/525	0.064	S : AB : SE = 50 : 20 : 30	$80Li_2S \cdot 20P_2S_5$	1.3–3.3	12.7	[50f]
S-carbon-SE	BM	1568/784 1096/548	0.64 6.4	S : KB : SE = 50 : 10 : 40	$Li_{1.5}PS_{3.3}$/LGPS	1.1–3.1	9.5	[50d]
S-AC-SE[a]	BM	1600/800	1.3	S : AC : SE = 50 : 10 : 40	$Li_{1.5}PS_{3.3}$/LGPS	1.1–3.1	9.5	[50e]
S-carbon	Gas-phase mixing	900/225 380/95	0.013 0.13	S : AB : SE = 25 : 25 : 50	$Li_{3.75}Ge_{0.25}P_{0.75}S_4$	1.1–3.3	6.4	[50a]
S-MesoC[b]	Gas-phase mixing	1900/264	0.13	S-MesoC : SE = 50 : 50	$Li_{3.75}Ge_{0.25}P_{0.75}S_4$	1.0–3.4	6.4	[50c]
S-PAN	HT	835/315	0.038	S-PAN : AB : SE = 20 : 3 : 30[e]	$Li_2S \cdot P_2S_5$	1.0–3.0	7.5	[52]
Li_2S@Li_3PS_4	Wet method	848/260[c]	0.02	Li_2S@Li_3PS_4 : C : PVC = 65 : 25 : 10	β-Li_3PS_4	0.2–0.5	0.16–0.40	[14g]

[a] AC: activated carbon. [b] MesoC: mesoporous carbon. [c] Calculated from $Li_2S : P_2S_5 = 10 : 1$ mole ratio. [d] S or Li_2S : Cu = 3 : 1 wt. ratio. [e] S : PAN = 45 : 55 wt. ratio. [f] AB: acetylene black; KB: ketjen black.

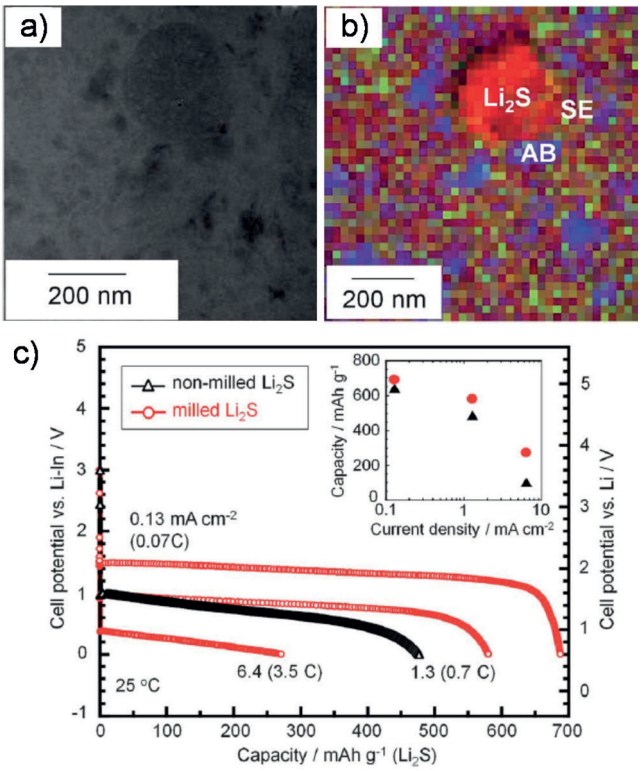

Figure 9. a) Cross-sectional HAADF-STEM image; and b) corresponding electron energy loss spectroscopy (EELS) map for Li_2S composite electrodes. c) Discharge voltage profiles of Li_2S composite electrodes in ASLBs. Adapted with permission from Ref. [14a].

proposed to be the main factor for the reactivity of sulfur.[44e] Copper was also proposed as an alternative to carbon for the fabrication of nanocomposites containing sulfur or Li_2S, although the performance was poorer than the one found for composite materials containing carbon.[51] Lee and co-workers reported that polyacrylonitrile (PAN)-sulfur exhibited a discharge capacity of 835 mA h (g of S)$^{-1}$ in ASLBs operating at 60 °C.[52] The nanosized Li_2S encapsulated in the ion-conducting β-Li_3PS_4, named as lithium superionic sulfide (LSS), was synthesized by a wet method, with sulfur being reduced by lithium triethylborohydride ($LiEt_3BH$) in tetrahydrofuran (THF), and it appeared to outperform the simple Li_2S nanocrystal electrode when tested in ASLBs.[14g]

5.4. Reinvestigated or New Electrode Materials

Besides the aforementioned electrode materials based on Li metal, Li_xMO_2, and sulfur or Li_2S, other electrode materials typical of LIBs, such as graphite,[53–55] spinel-structure $Li_4Ti_5O_{12}$ (LTO),[56] Si-based materials,[42ae,57,58] metal oxides such as Fe_2O_3,[59] metal phosphides (e.g., Sn_4P_3, NiP_2),[60] and olivine-structure $LiFePO_4$,[61] have been tested for ASLBs. Because of the low operating potential, the performance of graphite is highly dependent on the electrochemical stability of the SEs.[54] The bilayer structure featuring two different SEs optimized the electrochemical performance of ASLB.[54] Li-alloy materials,

Israel Journal of Chemistry

such as In and Al, can be good alternatives to replace lithium metal in ASLBs. All-solid-state test cells, using an Li-In alloy electrode as the counter/reference electrode, are frequently used.[3a,5a,14d,f] Those are similar to the conventional LE-based half-cells using lithium metal in that Li-In alloy provides an excess lithium source, a flat voltage plateau at 0.62 V (vs. Li/Li^+) for the range of $0<x<1$ in Li_xIn, and fast charge transfer kinetics.[42b,62] Li-Al alloy (0.38 V vs. Li/Li^+) has been also examined for ASLBs.[50c,63]

Notably, ASLBs provide a new opportunity to investigate, under a different perspective, electrode materials that were found inappropriate or simply not good enough for conventional LIBs. Lithium intercalation-deintercalation in the layered transition metal chalcogenides was extensively investigated in the early 1970s.[2c,64] However, transition metal chalcogenides were abandoned after the emergence of Li_xMO_2, which is lighter and allows operation at higher voltages than sulfides.[2a,c] However, the transition metal sulfides may be revisited for ASLBs because of their mild operating voltages (~2–3 V vs. Li/Li^+) and potentially good compatibility between different types of sulfides, creating an effective interface.[14e,f] In particular, TiS_2[14b,f] and Li_xTiS_2[65] were reported to show good cycling performance in ASLBs, with reversible capacities close to the theoretical one ($TiS_2+Li^++e^-\leftrightarrow LiTiS_2$, 239 mA h g^{-1}). The Chevrel-phase compound, $(Cu_x)Mo_6S_{8-y}$, also exhibited excellent cycle life in ASLBs.[5b,c] The outstanding performance of TiS_2 and $(Cu_x)Mo_6S_{8-y}$ is associated with their metallic nature, their reversible intercalation/deintercalation, high Li^+ ion diffusivity, and so on.[5b,c,14b,f,65] Lee and co-workers investigated the electrochemical reactivity of pyrite FeS_2 in ASLBs.[14c] In the LE cells, FeS_2 exhibited an initial capacity of ~500 mA h g^{-1} at 30 °C and a rapid capacity fading, as shown in Figure 10.[14c] Its performance became even worse at 60 °C. The poor performance of FeS_2 is associated with the dissolution of intermediate polysulfide products into the LEs.[14c] In sharp contrast, FeS_2 with a sulfide SE reacts reversibly with lithium, showing excellent cyclability, as shown in Figure 10. Jung and co-workers reported that $LiTi_2(PS_4)_3$ worked much better in ASLBs than in cells featuring a LE.[14e] The poorer performance shown by $LiTi_2(PS_4)_3$ in the previous reports[66] were associated with its dissolution into the LE.[2a,14e] The amorphous titanium polysulfide prepared by a mechanochemical method is promising for ASLBs, contrary to what was found in the case of LE cells.[67] The aforementioned materials present not only large capacities, overcoming the limit in capacity, typical of conventional cathode materials such as Li_xMO_2, but they are also less subject to dimensional changes compared with the elemental sulfur-based electrodes, thereby becoming alternative promising electrode materials for ASLBs.

Liang and co-workers reported the unique synthesis of β-Li_3PS_4 SE, with an ionic conductivity of 1.5×10^{-4} S cm^{-1} at RT, using a wet chemical method based on THF.[68] Lithium polysulfidophosphate (LPSP, Li_3PS_{4+n}) was also prepared by a wet chemical method and was tested as a cathode material for ASLBs.[14h] The proposed mechanism for the formation of LPSP and for the electrochemical reaction of LPSP with lithium are shown in Figure 11.[14h] LPSP showed an initial discharge capacity of 1272 mA h g^{-1} (based on the incorporated sulfur content) at RT.[14h]

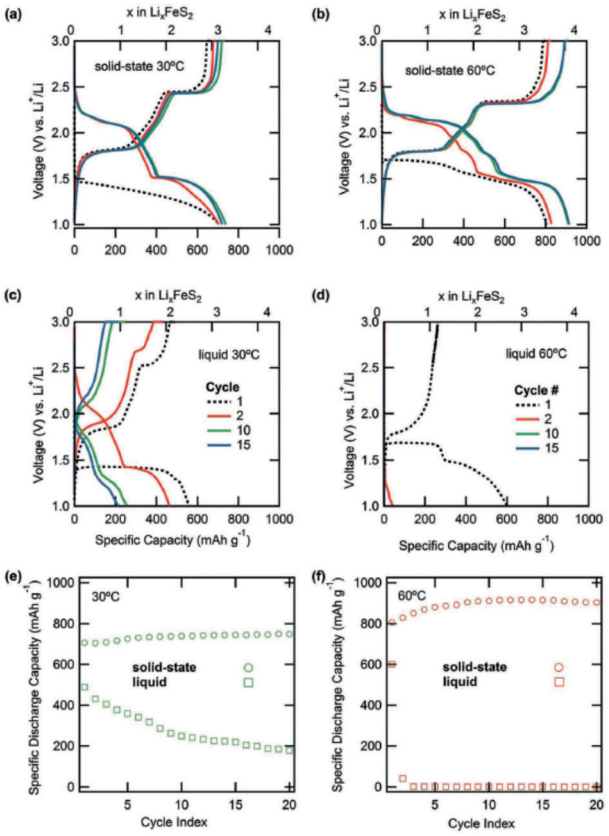

Figure 10. Comparison of electrochemical performance of FeS_2 at 30 °C and 60 °C in conventional liquid cells and in solid-state cells. Adapted with permission from Ref. [14c].

6. Design of Composite Electrodes

Achieving a good electrical connection between the current collector and each of the active materials is of prime importance in the fabrication of a composite electrode, not only for conventional LIBs,[2b] but also for ASLBs. For example, the electrochemical performance of $LiCoO_2$ in ASLBs is significantly affected by the conductive additives.[42j,k] In the case of ASLBs, however, the design of composite electrodes is more complicated than for LIBs because many factors contribute to significantly affect the ionic conduction pathways, including morphology, percolation of SEs, and contacts between the active materials and the SE. For example, the capacity of $LiCoO_2$/In solid-

Israel Journal of Chemistry

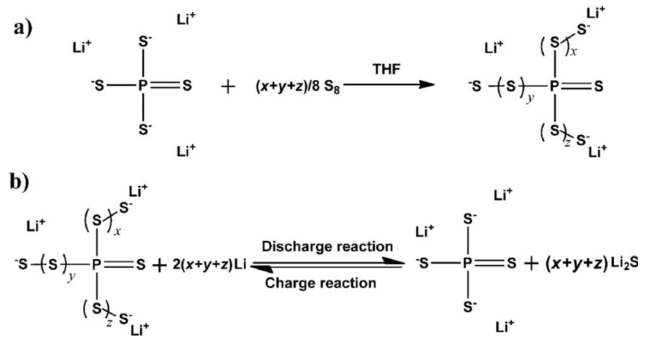

Figure 11. a) Formation of lithium polysulfidophosphate (LPSP, Li_3PS_{4+n}, $n=(x+y+z)/3$) by reaction of sulfur with Li_3PS_4 in THF. b) Electrochemical reaction mechanism for the charge and discharge of LPSP, indicating reversible scission and formation of S-S bonds in LPSP. Adapted with permission from Ref. [14h].

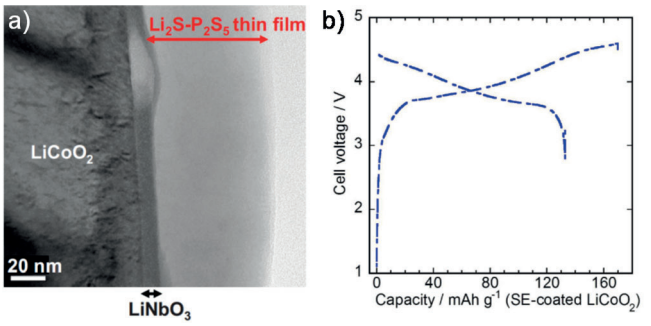

Figure 12. a) Cross-sectional TEM image of the $Li_2S{\cdot}P_2S_5$ SE-coated $LiCoO_2$ particles by pulsed laser deposition. b) Charge-discharge curves of an ASLB consisting of an $LiCoO_2$ positive electrode coated with $Li_2S{\cdot}P_2S_5$ SE, a graphite negative electrode coated with $Li_2S{\cdot}P_2S_5$ SE, and a $Li_2S{\cdot}P_2S_5$ SE layer. Adapted with permission from Refs. [9, 69a].

state cells is highly dependent on the composition of the composite electrodes.[42j] In contrast, LEs can easily be absorbed into the porous structure of composite electrodes in LIBs, wetting almost all the exposed surfaces of the active materials.

In the majority of publications regarding the composite electrodes of Li_xMO_2, such as $LiCoO_2$, a 30–65 wt % of SEs is included to ensure the creation of facile ionic conduction pathways.[3a,5a,9,14d,23b,c,32,36,41–43] Obviously, the very high content of SEs may severely reduce the energy density of ASLBs. To overcome this issue, the ideal structure of the composite electrode should contain the active materials coated by layers of SE as uniform as possible, with electronic wiring provided by carbon additives. Tatsumisago and co-workers reported that a thin $Li_2S{\cdot}P_2S_5$ SE film can be deposited on electrode materials by pulsed laser deposition (PLD), as shown in Figure 12a.[69] As a proof of concept, the authors successfully demonstrated that an ASLB fabricated with the SE-coated $LiCoO_2$ could work without any addition of SE powders to the positive electrode layer.[9,69b] The promising result of 133 mA h (g of $LiCoO_2$)$^{-1}$ for discharge capacity was obtained using a $LiCoO_2$/graphite full cell in which 10 wt % of the SE was coated in each electrode by PLD, as shown in Figure 12b.[9] However, as the expensive PLD technique is far from being a viable solution for practical applications, innovative approaches are needed. Wet coating of $Li_2S{\cdot}P_2S_5$ SE using N-methyl formamide, which has the advantage of fully dissolving $Li_2S{\cdot}P_2S_5$, was tried.[42ad] However, the improvement in the performance of the cell was not significant, since the conductivity was only 2.6×10^{-6} S cm^{-1}.[42ad] It was also demonstrated that a much higher conductivity (1.82×10^{-4} S cm^{-1}) could be obtained for thio-LISICON-like $Li_{3.25}Ge_{0.25}P_{0.75}S_4$ using Li_2S, P_2S_5, and GeS_2 as precursors, and employing a solution method with anhydrous hydrazine.[70] However, anhydrous hydrazine is extremely dangerous, thus discouraging further developments.

Although the two dimensional contacts between the active materials and the sulfide SEs are simply made by cold pressing,[3b,9] it is worth noting that hot pressing at temperatures above the glass transition temperature can deform and enable the merging of the SE sulfide particles, forming poreless, dense pellets (Figure 13a and Figure 13b).[4,9,42v] Consequently, hot pressing of composite electrodes containing sulfide SEs resulted in an increased utilization of the active materials in the ASLBs, as demonstrated in the case of $Li_4Ti_5O_{12}$.[42v] However, the trade-off of hot pressing is the massive interfacial reaction observed in the case of $LiCoO_2$.[42v] A protective coating on $LiCoO_2$ by $LiNbO_3$ may partially suppress the interfacial reaction occurring during hot pressing.[42v] Figure 13c shows that a full-cell made of $Li_4Ti_5O_{12}$/$80Li_2S{\cdot}20P_2S_5$ glass/$LiNbO_3$-coated $LiCoO_2$, prepared by hot pressing at 210 °C, outperforms the cell prepared by cold pressing.[42v]

As found in the literature for sulfur or Li_2S for ASLBs, the mechanochemical method is a versatile and scalable process for achieving ideal nanocomposite structures for ASLBs.[14a,50b,d–f] This is also the case for other electrode

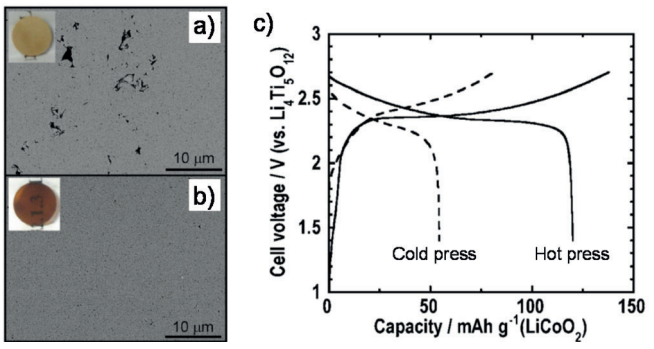

Figure 13. SEM images of cross sections of $80Li_2S{\cdot}20P_2S_5$ glassy SE prepared by a) cold pressing; and by b) hot pressing at 200 °C. The photographs of pellets are shown in the insets. c) First charge-discharge voltage profiles of the $Li_4Ti_5O_{12}$/$80Li_2S{\cdot}20P_2S_5$ glass/$LiNbO_3$-coated $LiCoO_2$ full cells prepared by hot press and cold press. Adapted with permission from Refs. [9, 42v].

materials for ASLBs.[14f,71] For instance, nanosized NiS electrodes can be prepared by the following consecutive reactions, using the mechanochemical method:[71a]

$$Ni_3S_2 + Li_3N \rightarrow Ni + Li_2S + N_2 \uparrow$$

$$Ni + Li_2S + S + P_2S_5 \rightarrow NiS_2 + Li_2S \cdot P_2S_5$$

The as-prepared NiS nanocomposite electrode exhibits increased capacity, compared with the simple mixture electrode.[71a] Using a similar approach, Lee and co-workers synthesized a pyrite FeS_2 nanocomposite electrode by the following successive mechanochemical and thermal treatments of Fe_2P, S, and Li_2S:[71b]

$$2Fe_2P + 13S \rightarrow 4FeS_2 + P_2S_5 \ (350\,^{\circ}C)$$

$$22.5(4FeS_2 + P_2S_5) + 77.5Li_2S \rightarrow$$
$$90FeS_2 + 77.5Li_2S \cdot 22.5P_2S_5$$

Jung and co-workers investigated the effect of the mechanochemical reaction between TiS_2 and Li_3PS_4 and observed abnormally increased Li^+ storage.[14f] In Figure 14a–14f, as the BM time increases, the extra capacity also increases. After 9 min of BM, the nanocomposite electrode exhibits 837 mA h (g of TiS_2)$^{-1}$ in the voltage range of 1.0–3.0 V, as shown in Figure 14f.[14f] The significantly increased capacity in the nanocomposite electrode probably originated from the amorphous Li-Ti-P-S phase formed by the partial reaction between TiS_2 and the SE occurring during BM, as shown in Figure 14g and Figure 14h.[14f]

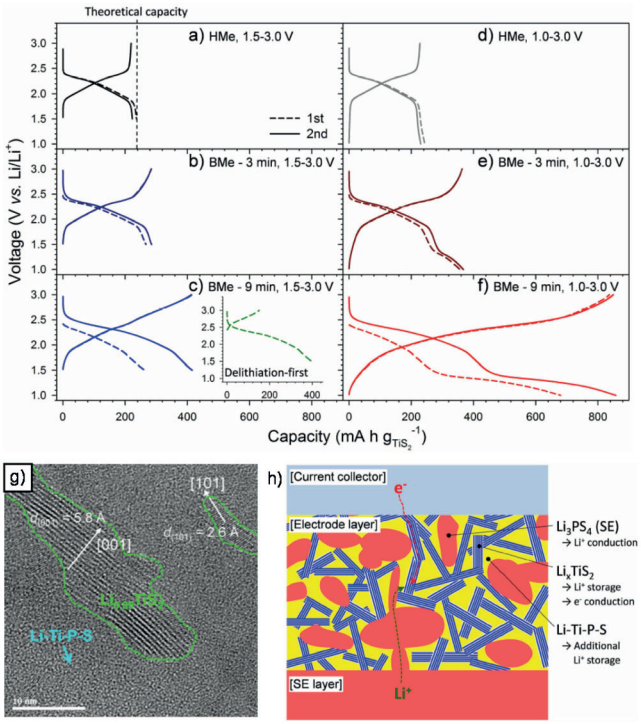

Figure 14. a)–f) First two charge-discharge voltage curves of hand-mixed (HMe) and ball-milled electrodes (BMe) of TiS_2-based nanocomposite electrodes. g) Cross-sectional HRTEM image of BMe. h) Schematic diagram of BMe showing the nanostructures and the roles of each components. Adapted with permission from Ref. [14f].

7. Summary and Outlook

In summary, we provide an overview on the progress made on sulfide SEs and bulk-type ASLBs. The ductility and the high ionic conductivity at RT (~10^{-2} S cm^{-1}) by the sulfide SEs at their best performance are exceptional properties, allowing the realization of high-energy bulk-type ASLBs, using a scalable process, in the near future. However, the success of ASLBs using sulfide SE cannot be guaranteed without further innovations to address specific key points that were extensively discussed in this review, as shown in Figure 15. These include:

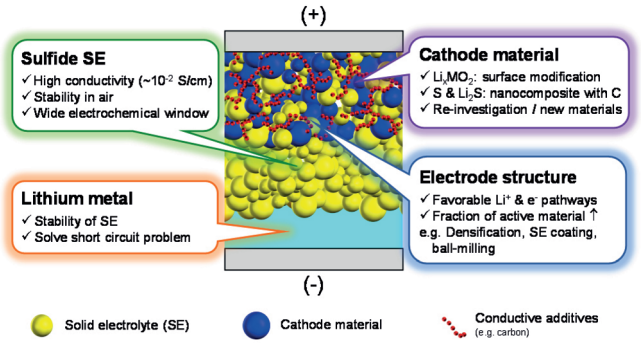

Figure 15. Schematic diagram showing the summary of issues and challenges in development of high-performance bulk-type ASLB using sulfide SEs.

- Design of advanced sulfide SEs in terms of composition and structure. In particular, requirements of high ionic conductivity, wide electrochemical windows, and resistivity to water-induced decomposition should be met.
- Understanding of the phenomena occurring at the interface between electrode materials and SEs. This will shed light on possible strategies to adopt to address problems due to the incompatibility between different materials, as shown in the case of the Li_xMO_2 cathode, whose performance was improved by surface modifications induced by an electron-insulating, ionic-conducting metal oxide coating or an electron-conducting metal sulfide coating.
- The privileged opportunity to use lithium metal as the anode and sulfur or Li_2S as the cathode for achieving the ultimate energy density.
- The (re)investigation of electrode materials, to provide more options for ASLBs, as shown, for example, in the cases of FeS_2 and $LiTi_2(PS_4)_3$.

- The new strategies to adopt for the synthesis and the fabrication of nanostructures used in the composite electrodes for ASLBs. Examples include mechanochemical methods for sulfide active materials and SEs, and solution methods for new sulfide compounds.

Recently, high ionic conductivity of cations in sulfides was also found for non-Li sulfide compounds. The cubic structure Na_3PS_4 exhibited conductivity of over 10^{-4} S cm^{-1} at RT.[3b,72] If further development of Na-ion conductive sulfide SEs is to be carried out and higher ionic conductivity is to be achieved, a new era of all-solid-state Na batteries could begin.[73] The exploration of Mg-conducting sulfide materials, such as $MgS \cdot P_2S_5 \cdot MgI_2$ glass,[74] is also in line with the aforementioned research trends for new generation batteries.[73,75]

Most of the efforts made in the field of ASLBs so far have been limited to the investigation of materials chemistry issues, with only a few reports made on more practical aspects.[76] Nowadays, an increased flexibility in the design of LIBs has become a hot issue, as is confirmed by the rapid progress of flexible batteries.[77] On a similar basis, it is expected that eventually more engineering issues will appear for the fabrication of several typologies of ASLBs using a scalable process.

Acknowledgements

This work was supported by the Energy Efficiency and Resources Program of the Korea Institute of Energy Technology Evaluation and Planning (KETEP) grant funded by the Korea government Ministry of Trade, Industry and Energy (No. 20112010100150) and by Basic Science Research Program through the National Research Foundation of Korea (NRF) funded by the Ministry of Education (No. 2014058760).

References

[1] T. Agura, K. Tozawa, *Prog. Batt. Solar Cells* **1990**, *9*, 209–217.
[2] a) J. B. Goodenough, Y. Kim, *Chem. Mater.* **2010**, *22*, 587–603; b) J.-M. Tarascon, *Philos. Trans. R. Soc. A* **2010**, *368*, 3227–3241; c) M. S. Whittingham, *Chem. Rev.* **2004**, *104*, 4271–4301; d) K. Xu, *Chem. Rev.* **2004**, *104*, 4303–4417.
[3] a) N. Kamaya, K. Homma, Y. Yamakawa, M. Hirayama, R. Kanno, M. Yonemura, T. Kamiyama, Y. Kato, S. Hama, K. Kawamoto, A. Mitsui, *Nat. Mater.* **2011**, *10*, 682–686; b) A. Hayashi, K. Noi, A. Sakuda, M. Tatsumisago, *Nat. Commun.* **2012**, *3*, 856; c) G. Y. Adachi, N. Imanaka, H. Aono, *Adv. Mater.* **1996**, *8*, 127–135.
[4] Y. Seino, T. Ota, K. Takada, A. Hayashi, M. Tatsumisago, *Energy Environ. Sci.* **2014**, *7*, 627–631.
[5] a) A. Sakuda, A. Hayashi, M. Tatsumisago, *Chem. Mater.* **2010**, *22*, 949–956; b) M. Nagao, H. Kitaura, A. Hayashi, M. Tatsumisago, *J. Power Sources* **2009**, *189*, 672–675; c) M. Nagao, H. Kitaura, A. Hayashi, M. Tatsumisago, *J. Electrochem. Soc.* **2013**, *160*, A819–A823.
[6] a) T. Abe, H. Fukuda, Y. Iriyama, Z. Ogumi, *J. Electrochem. Soc.* **2004**, *151*, A1120–A1123; b) M. Chiku, W. Tsujiwaki, E. Higuchi, H. Inoue, *Electrochemistry* **2012**, *80*, 740–742.
[7] a) B. Wang, J. B. Bates, F. X. Hart, B. C. Sales, R. A. Zuhr, J. D. Robertson, *J. Electrochem. Soc.* **1996**, *143*, 3203–3213; b) J. B. Bates, N. J. Dudney, B. Neudecker, A. Ueda, C. D. Evans, *Solid State Ionics* **2000**, *135*, 33–45.
[8] A. Patil, V. Patil, D. W. Shin, J.-W. Choi, D.-S. Paik, S.-J. Yoon, *Mater. Res. Bull.* **2008**, *43*, 1913–1942.
[9] A. Sakuda, A. Hayashi, M. Tatsumisago, *Sci. Rep.* **2013**, *3*, 2261.
[10] a) R. Kanno, M. Murayama, *J. Electrochem. Soc.* **2001**, *148*, A742–A746; b) F. Mizuno, A. Hayashi, K. Tadanaga, M. Tatsumisago, *Adv. Mater.* **2005**, *17*, 918–921; c) T. Lapp, S. Skaarup, A. Hooper, *Solid State Ionics* **1983**, *11*, 97–103; d) G. Sahu, Z. Lin, J. Li, Z. Liu, N. Dudney, C. Liang, *Energy Environ. Sci.* **2014**, *7*, 1053–1058; e) P. Knauth, *Solid State Ionics* **2009**, *180*, 911–916; f) S. Stramare, V. Thangadurai, W. Weppner, *Chem. Mater.* **2003**, *15*, 3974–3990; g) H. Aono, E. Sugimoto, *J. Electrochem. Soc.* **1989**, *136*, 590–591; h) R. Murugan, V. Thangadurai, W. Weppner, *Angew. Chem. Int. Ed.* **2007**, *46*, 7778–7781.
[11] a) M. Kotobuki, H. Munakata, K. Kanamura, Y. Sato, T. Yoshida, *J. Electrochem. Soc.* **2010**, *157*, A1076–A1079; b) K. H. Kim, Y. Iriyama, K. Yamamoto, S. Kumazaki, T. Asaka, K. Tanabe, C. A. J. Fisher, T. Hirayama, R. Murugan, Z. Ogumi, *J. Power Sources* **2011**, *196*, 764–767.
[12] A. Aboulaich, R. Bouchet, G. Delaizir, V. Seznec, L. Tortet, M. Morcrette, P. Rozier, J.-M. Tarascon, V. Viallet, *Adv. Energy Mater.* **2011**, *1*, 179–183.
[13] S. Ohta, J. Seki, Y. Yagi, Y. Kihira, T. Tani, T. Asoka, *J. Power Sources* **2014**, *265*, 40–44.
[14] a) M. Nagao, A. Hayashi, M. Tatsumisago, *J. Mater. Chem.* **2012**, *22*, 10015–10020; b) J. E. Trevey, C. R. Stoldt, S.-H. Lee, *J. Electrochem. Soc.* **2011**, *158*, A1282–A1289; c) T. A. Yersak, H. A. Macpherson, S. C. Kim, V.-D. Le, C. S. Kang, S.-B. Son, Y.-H. Kim, J. E. Trevey, K. H. Oh, C. Stoldt, S.-H. Lee, *Adv. Energy Mater.* **2013**, *3*, 120–127; d) N. Ohta, K. Takada, L. Zhang, R. Ma, M. Osada, T. Sasaki, *Adv. Mater.* **2006**, *18*, 2226–2229; e) B. R. Shin, Y. S. Jung, *J. Electrochem. Soc.* **2014**, *161*, A154–A159; f) B. R. Shin, Y. J. Nam, J. W. Kim, Y.-G. Lee, Y. S. Jung, *Sci. Rep.* **2014**, *4*, 5572; g) Z. Lin, Z. Liu, N. J. Dudney, C. Liang, *ACS Nano* **2013**, *7*, 2829–2833; h) Z. Lin, Z. Liu, W. Fu, N. J. Dudney, C. Liang, *Angew. Chem. Int. Ed.* **2013**, *52*, 7460–7463.
[15] A. R. West, *Basic Solid State Chemistry*, 2nd Edition, John Wiley & Sons, Chichester, **1999**.
[16] Y. Mo, S. P. Ong, G. Ceder, *Chem. Mater.* **2012**, *24*, 15–17.
[17] A. Kuhn, J. Koehler, B. V. Lotsch, *Phys. Chem. Chem. Phys.* **2013**, *15*, 11620–11622.
[18] S. P. Ong, Y. Mo, W. D. Richards, L. Miara, H. S. Lee, G. Ceder, *Energy Environ. Sci.* **2013**, *6*, 148–156.
[19] P. Bron, S. Johansson, K. Zick, J. S. auf der Guenne, S. Dehnen, B. Roling, *J. Am. Chem. Soc.* **2013**, *135*, 15694–15697.
[20] T. Kaib, S. Haddadpour, M. Kapitein, P. Bron, C. Schroeder, H. Eckert, B. Roling, S. Dehnen, *Chem. Mater.* **2012**, *24*, 2211–2219.
[21] a) A. Hayashi, S. Hama, T. Minami, M. Tatsumisago, *Electrochem. Commun.* **2003**, *5*, 111–114; b) M. Tatsumisago, F. Mizuno, A. Hayashi, *J. Power Sources* **2006**, *159*, 193–199; c) F. Mizuno, A. Hayashi, K. Tadanaga, M. Tatsumisago,

Solid State Ionics **2006**, *177*, 2721–2725; d) K. Minami, F. Mizuno, A. Hayashi, M. Tatsumisago, *Solid State Ionics* **2007**, *178*, 837–841; e) A. Hayashi, K. Minami, S. Ujiie, M. Tatsumisago, *J. Non-Cryst. Solids* **2010**, *356*, 2670–2673; f) Y. Kowada, M. Tatsumisago, T. Minami, H. Adachi, *J. Non-Cryst. Solids* **2008**, *354*, 360–364.

[22] K. Minami, A. Hayashi, M. Tatsumisago, *J. Non-Cryst. Solids* **2010**, *356*, 2666–2669.

[23] a) H.-J. Deiseroth, S.-T. Kong, H. Eckert, J. Vannahme, C. Reiner, T. Zaiss, M. Schlosser, *Angew. Chem. Int. Ed.* **2008**, *47*, 755–758; b) S. Boulineau, M. Courty, J.-M. Tarascon, V. Viallet, *Solid State Ionics* **2012**, *221*, 1–5; c) S. Boulineau, J.-M. Tarascon, J.-B. Leriche, V. Viallet, *Solid State Ionics* **2013**, *242*, 45–48.

[24] Z. M. Zhang, J. H. Kennedy, *Solid State Ionics* **1990**, *38*, 217–224.

[25] R. Sakamoto, M. Tatsumisago, T. Minami, *J. Phys. Chem. B* **1999**, *103*, 4029–4031.

[26] R. Mercier, J. P. Malugani, B. Fahys, G. Robert, *Solid State Ionics* **1981**, *5*, 663–666.

[27] a) J. H. Kennedy, Z. Zhang, *J. Electrochem. Soc.* **1988**, *135*, 859–862; b) J. H. Kennedy, Z. Zhang, *Solid State Ionics* **1988**, *28*, 726–728.

[28] T. Minami, A. Hayashi, M. Tatsumisago, *Solid State Ionics* **2006**, *177*, 2715–2720.

[29] M. Ribes, B. Barrau, J. L. Souquet, *J. Non-Cryst. Solids* **1980**, *38–9*, 271–276.

[30] H. Wada, M. Menetrier, A. Levasseur, P. Hagenmuller, *Mater. Res. Bull.* **1983**, *18*, 189–193.

[31] H. Muramatsu, A. Hayashi, T. Ohtomo, S. Hama, M. Tatsumisago, *Solid State Ionics* **2011**, *182*, 116–119.

[32] T. Ohtomo, A. Hayashi, M. Tatsumisago, K. Kawamoto, *Electrochemistry* **2013**, *81*, 428–431.

[33] T. Ohtomo, A. Hayashi, M. Tatsumisago, K. Kawamoto, *J. Mater. Sci.* **2013**, *48*, 4137–4142.

[34] a) Y. S. Jung, A. S. Cavanagh, A. C. Dillon, M. D. Groner, S. M. George, S. H. Lee, *J. Electrochem. Soc.* **2010**, *157*, A75–A81; b) Y. S. Jung, A. S. Cavanagh, L. A. Riley, S. H. Kang, A. C. Dillon, M. D. Groner, S. M. George, S. H. Lee, *Adv. Mater.* **2010**, *22*, 2172–2176; c) Y. S. Jung, P. Lu, A. S. Cavanagh, C. Ban, G. H. Kim, S. H. Lee, S. M. George, S. J. Harris, A. C. Dillon, *Adv. Energy Mater.* **2013**, *3*, 213–219.

[35] B. R. Shin, Y. J. Nam, D. Y. Oh, D. H. Kim, J. W. Kim, Y. S. Jung, *Electrochim. Acta* **2014**, *146*, 395–402.

[36] a) A. Sakuda, H. Kitaura, A. Hayashi, K. Tadanaga, M. Tatsumisago, *J. Electrochem. Soc.* **2009**, *156*, A27–A32; b) J. E. Trevey, Y. S. Jung, S.-H. Lee, *Electrochim. Acta* **2011**, *56*, 4243–4247.

[37] a) D. W. Murphy, J. N. Carides, F. J. D. Salvo, C. Cros, J. V. Waszczak, *Mater. Res. Bull.* **1977**, *12*, 825–830; b) Y. Kim, J. B. Goodenough, *Electrochem. Solid-State Lett.* **2009**, *12*, A73–A75.

[38] a) G. Girishkumar, B. McCloskey, A. C. Luntz, S. Swanson, W. Wilcke, *J. Phys. Chem. Lett.* **2010**, *1*, 2193–2203; b) X. L. Ji, K. T. Lee, L. F. Nazar, *Nat. Mater.* **2009**, *8*, 500–506.

[39] D. Aurbach, E. Zinigrad, Y. Cohen, H. Teller, *Solid State Ionics* **2002**, *148*, 405–416.

[40] M. Nagao, A. Hayashi, M. Tatsumisago, T. Kanetsuku, T. Tsuda, S. Kuwabata, *Phys. Chem. Chem. Phys.* **2013**, *15*, 18600–18606.

[41] M. Nagao, A. Hayashi, M. Tatsumisago, *Electrochemistry* **2012**, *80*, 734–736.

[42] a) K. Iwamoto, N. Aotani, K. Takada, S. Kondo, *Solid State Ionics* **1995**, *79*, 288–291; b) K. Takada, N. Aotani, K. Iwamoto, S. Kondo, *Solid State Ionics* **1996**, *86*, 877–882; c) R. Komiya, A. Hayashi, H. Morimoto, M. Tatsumisago, T. Minami, *Solid State Ionics* **2001**, *140*, 83–87; d) A. Hayashi, H. Yamashita, M. Tatsumisago, T. Minami, *Solid State Ionics* **2002**, *148*, 381–389; e) M. Murayama, R. Kanno, M. Irie, S. Ito, T. Hata, N. Sonoyama, Y. Kawamoto, *J. Solid State Chem.* **2002**, *168*, 140–148; f) A. Hayashi, R. Komiya, M. Tatsumisago, T. Minami, *Solid State Ionics* **2002**, *152*, 285–290; g) M. Tatsumisago, *Solid State Ionics* **2004**, *175*, 13–18; h) F. Mizuno, A. Hayashi, K. Tadanaga, T. Minami, M. Tatsumisago, *Solid State Ionics* **2004**, *175*, 699–702; i) A. Hayashi, S. Hama, F. Mizuno, K. Tadanaga, T. Minami, M. Tatsumisago, *Solid State Ionics* **2004**, *175*, 683–686; j) F. Mizuno, A. Hayashi, K. Tadanaga, M. Tatsumisago, *J. Power Sources* **2005**, *146*, 711–714; k) F. Mizuno, A. Hayashi, K. Tadanaga, M. Tatsumisago, *J. Electrochem. Soc.* **2005**, *152*, A1499–A1503; l) T. Ohtomo, F. Mizuno, A. Hayashi, K. Tadanaga, M. Tatsumisago, *J. Power Sources* **2005**, *146*, 715–718; m) F. Mizuno, A. Hayashi, K. Tadanaga, M. Tatsumisago, *Solid State Ionics* **2006**, *177*, 2731–2735; n) N. Ohta, K. Takada, I. Sakaguchi, L. Zhang, R. Ma, K. Fukuda, M. Osada, T. Sasaki, *Electrochem. Commun.* **2007**, *9*, 1486–1490; o) T. Konishi, A. Hayashi, K. Tadanaga, T. Minami, M. Tatsumisago, *J. Non-Cryst. Solids* **2008**, *354*, 380–385; p) M. Tatsumisago, A. Hayashi, *J. Non-Cryst. Solids* **2008**, *354*, 1411–1417; q) H. Okamoto, S. Hikazudani, C. Inazumi, T. Takeuchi, M. Tabuchi, K. Tatsumi, *Electrochem. Solid-State Lett.* **2008**, *11*, A97–A100; r) A. Sakuda, H. Kitaura, A. Hayashi, K. Tadanaga, M. Tatsumisago, *J. Power Sources* **2009**, *189*, 527–530; s) A. Sakuda, A. Hayashi, M. Tatsumisago, *J. Power Sources* **2010**, *195*, 599–603; t) J. E. Trevey, Y. S. Jung, S.-H. Lee, *J. Power Sources* **2010**, *195*, 4984–4989; u) X. Xu, K. Takada, K. Watanabe, I. Sakaguchi, K. Akatsuka, B. T. Hang, T. Ohnishi, T. Sasaki, *Chem. Mater.* **2011**, *23*, 3798–3804; v) H. Kitaura, A. Hayashi, T. Ohtomo, S. Hama, M. Tatsumisago, *J. Mater. Chem.* **2011**, *21*, 118–124; w) Y. Kato, K. Kawamoto, R. Kanno, M. Hirayama, *Electrochemistry* **2012**, *80*, 749–751; x) J. H. Woo, J. E. Trevey, A. S. Cavanagh, Y. S. Choi, S. C. Kim, S. M. George, K. H. Oh, S.-H. Lee, *J. Electrochem. Soc.* **2012**, *159*, A1120–A1124; y) Y. Ooura, N. Machida, M. Naito, T. Shigematsu, *Solid State Ionics* **2012**, *225*, 350–353; z) A. Sakuda, N. Nakamoto, H. Kitaura, A. Hayashi, K. Tadanaga, M. Tatsumisago, *J. Mater. Chem.* **2012**, *22*, 15247–15254; aa) K. Takada, N. Ohta, L. Zhang, X. Xu, H. Bui Thi, T. Ohnishi, M. Osada, T. Sasaki, *Solid State Ionics* **2012**, *225*, 594–597; ab) K. Takada, *Langmuir* **2013**, *29*, 7538–7541; ac) T. Ohtomo, A. Hayashi, M. Tatsumisago, Y. Tsuchida, S. Hama, K. Kawamoto, *J. Power Sources* **2013**, *233*, 231–235; ad) S. Teragawa, K. Aso, K. Tadanaga, A. Hayashi, M. Tatsumisago, *J. Power Sources* **2014**, *248*, 939–942; ae) K. Okada, N. Machida, M. Naito, T. Shigematsu, S. Ito, S. Fujiki, M. Nakano, Y. Aihara, *Solid State Ionics* **2014**, *255*, 120–127.

[43] a) H. Kitaura, A. Hayashi, K. Tadanaga, M. Tatsumisago, *Electrochim. Acta* **2010**, *55*, 8821–8828; b) F. Mizuno, A. Hayashi, K. Tadanaga, T. Minami, M. Tatsumisago, *J. Power Sources* **2003**, *124*, 170–173; c) N. Machida, H. Maeda, H. Peng, T. Shigematsu, *J. Electrochem. Soc.* **2002**, *149*, A688–A693.

[44] J. Maier, *J. Phys. Chem. Solids* **1985**, *46*, 309–320.

[45] a) K. Takada, N. Ohta, L. Zhang, K. Fukuda, I. Sakaguchi, R. Ma, M. Osada, T. Sasaki, *Solid State Ionics* **2008**, *179*, 1333–1337; b) C. Yada, A. Ohmori, K. Ide, H. Yamasaki, T.

Kato, T. Saito, F. Sagane, Y. Iriyama, *Adv. Energy Mater.* **2014**, *4*, 1301416.
[46] a) J. Cho, Y. J. Kim, T. J. Kim, B. Park, *Angew. Chem. Int. Ed.* **2001**, *40*, 3367–3369; b) J. Cho, Y. W. Kim, B. Kim, J. G. Lee, B. Park, *Angew. Chem. Int. Ed.* **2003**, *42*, 1618–1621; c) C. Li, H. P. Zhang, L. J. Fu, H. Liu, Y. P. Wu, E. Rahmb, R. Holze, H. Q. Wu, *Electrochim. Acta* **2006**, *51*, 3872–3883; d) K. Leung, Y. Qi, K. R. Zavadil, Y. S. Jung, A. C. Dillon, A. S. Cavanagh, S. H. Lee, S. M. George, *J. Am. Chem. Soc.* **2011**, *133*, 14741–14754; e) Y. S. Jung, A. S. Cavanagh, L. Gedvilas, N. E. Widjonarko, I. D. Scott, S. H. Lee, G. H. Kim, S. M. George, A. C. Dillon, *Adv. Energy Mater.* **2012**, *2*, 1022–1027.
[47] X. Xu, K. Takada, K. Fukuda, T. Ohnishi, K. Akatsuka, M. Osada, H. Bui Thi, K. Kumagai, T. Sekiguchi, T. Sasaki, *Energy Environ. Sci.* **2011**, *4*, 3509–3512.
[48] a) Y. S. Jung, A. S. Cavanagh, Y. F. Yan, S. M. George, A. Manthiram, *J. Electrochem. Soc.* **2011**, *158*, A1298–A1302; b) E. Kang, Y. Jung, A. Cavanagh, G. Kim, S. George, A. Dillon, J. Kim, J. Lee, *Adv. Funct. Mater.* **2011**, *21*, 2430–2438; c) I. D. Scott, Y. S. Jung, A. S. Cavanagh, Y. F. An, A. C. Dillon, S. M. George, S. H. Lee, *Nano Lett.* **2011**, *11*, 414–418.
[49] S. M. George, *Chem. Rev.* **2010**, *110*, 111–131.
[50] a) T. Kobayashi, Y. Imade, D. Shishihara, K. Homma, M. Nagao, R. Watanabe, T. Yokoi, A. Yamada, R. Kanno, T. Tatsumi, *J. Power Sources* **2008**, *182*, 621–625; b) M. Nagao, A. Hayashi, M. Tatsumisago, *Electrochim. Acta* **2011**, *56*, 6055–6059; c) M. Nagao, Y. Imade, H. Narisawa, T. Kobayashi, R. Watanabe, T. Yokoi, T. Tatsumi, R. Kanno, *J. Power Sources* **2013**, *222*, 237–242; d) H. Nagata, Y. Chikusa, *J. Power Sources* **2014**, *263*, 141–144; e) H. Nagata, Y. Chikusa, *J. Power Sources* **2014**, *264*, 206–210; f) M. Nagao, A. Hayashi, M. Tatsumisago, *Energy Technol.* **2013**, *1*, 186–192.
[51] a) A. Hayashi, T. Ohtomo, F. Mizuno, K. Tadanaga, M. Tatsumisago, *Electrochem. Commun.* **2003**, *5*, 701–705; b) A. Hayashi, R. Ohtsubo, T. Ohtomo, F. Mizuno, M. Tatsumisago, *J. Power Sources* **2008**, *183*, 422–426; c) A. Hayashi, R. Ohtsubo, M. Tatsumisago, *Solid State Ionics* **2008**, *179*, 1702–1705.
[52] J. E. Trevey, J. R. Gilsdorf, C. R. Stoldt, S.-H. Lee, P. Liu, *J. Electrochem. Soc.* **2012**, *159*, A1019–A1022.
[53] K. Takada, S. Nakano, T. Inaba, A. Kjiyama, H. Sasaki, S. Kondo, M. Watanabe, *J. Electrochem. Soc.* **2003**, *150*, A274–A277.
[54] K. Takada, T. Inaba, A. Kajiyama, H. Sasaki, S. Kondo, M. Watanabe, M. Murayama, R. Kanno, *Solid State Ionics* **2003**, *158*, 269–274.
[55] T. Takeuchi, H. Kageyama, K. Nakanishi, T. Ohta, A. Sakuda, H. Sakaebe, H. Kobayashi, K. Tatsumi, Z. Ogumi, *ECS Electrochem. Lett.* **2014**, *3*, A31–A35.
[56] a) H. Kitaura, A. Hayashi, K. Tadanaga, M. Tatsumisago, *J. Electrochem. Soc.* **2009**, *156*, A114–A119; b) H. Kitaura, A. Hayashi, K. Tadanaga, M. Tatsumisago, *J. Power Sources* **2009**, *189*, 145–148.
[57] Y. Hashimoto, N. Machida, T. Shigematsu, *Solid State Ionics* **2004**, *175*, 177–180.
[58] a) J. Trevey, J. S. Jang, Y. S. Jung, C. R. Stoldt, S.-H. Lee, *Electrochem. Commun.* **2009**, *11*, 1830–1833; b) T. A. Yersak, S.-B. Son, J. S. Cho, S.-S. Suh, Y.-U. Kim, J.-T. Moon, K. H. Oh, S.-H. Lee, *J. Electrochem. Soc.* **2013**, *160*, A1497–A1501.
[59] a) H. Kitaura, K. Takahashi, F. Mizuno, A. Hayashi, K. Tadanaga, M. Tatsumisago, *J. Electrochem. Soc.* **2007**, *154*, A725–A729; b) H. Kitaura, K. Takahashi, F. Mizuno, A. Hayashi, K. Tadanaga, M. Tatsumisago, *J. Power Sources* **2008**, *183*, 418–421.
[60] a) A. Hayashi, A. Inoue, M. Tatsumisago, *J. Power Sources* **2009**, *189*, 669–671; b) A. Ueda, M. Nagao, A. Inoue, A. Hayashi, Y. Seino, T. Ota, M. Tatsumisago, *J. Power Sources* **2013**, *244*, 597–600.
[61] A. Sakuda, H. Kitaura, A. Hayashi, M. Tatsumisago, Y. Hosoda, T. Nagakane, A. Sakamoto, *Chem. Lett.* **2012**, *41*, 260–261.
[62] Y. S. Jung, K. T. Lee, J. H. Kim, J. Y. Kwon, S. M. Oh, *Adv. Funct. Mater.* **2008**, *18*, 3010–3017.
[63] R. Kanno, M. Murayama, T. Inaba, T. Kobayashi, K. Sakamoto, N. Sonoyama, A. Yamada, S. Kondo, *Electrochem. Solid-State Lett.* **2004**, *7*, A455–A458.
[64] M. S. Whittingham, *Science* **1976**, *192*, 1126–1127.
[65] a) T. A. Yersak, J. E. Trevey, S. H. Lee, *J. Power Sources* **2011**, *196*, 9830–9834; b) T. A. Yersak, Y. Yan, C. Stoldt, S.-H. Lee, *ECS Electrochem. Lett.* **2012**, *1*, A21–A23.
[66] Y. Kim, N. Arumugam, J. B. Goodenough, *Chem. Mater.* **2008**, *20*, 470–474.
[67] A. Sakuda, N. Taguchi, T. Takeuchi, H. Kobayashi, H. Sakaebe, K. Tatsumi, Z. Ogumi, *Solid State Ionics* **2014**, *262*, 143–146.
[68] a) Z. Liu, W. Fu, E. A. Payzant, X. Yu, Z. Wu, N. J. Dudney, J. Kiggans, K. Hong, A. J. Rondinone, C. Liang, *J. Am. Chem. Soc.* **2013**, *135*, 975–978; b) M. Gobet, S. Greenbaum, G. Sahu, C. Liang, *Chem. Mater.* **2014**, *26*, 3558–3564.
[69] a) A. Sakuda, A. Hayashi, T. Ohtomo, S. Hama, M. Tatsumisago, *Electrochem. Solid-State Lett.* **2010**, *13*, A73–A75; b) A. Sakuda, A. Hayashi, S. Hama, M. Tatsumisago, *J. Am. Ceram. Soc.* **2010**, *93*, 765–768.
[70] Y. Wang, Z. Liu, X. Zhu, Y. Tang, F. Huang, *J. Power Sources* **2013**, *224*, 225–229.
[71] a) A. Hayashi, Y. Nishio, H. Kitaura, M. Tatsumisago, *Electrochem. Commun.* **2008**, *10*, 1860–1863; b) T. A. Yersak, T. Evans, J. M. Whiteley, S.-B. Son, B. Francisco, K. H. Oh, S.-H. Lee, *J. Electrochem. Soc.* **2014**, *161*, A663–A667.
[72] A. Hayashi, K. Noi, N. Tanibata, M. Nagao, M. Tatsumisago, *J. Power Sources* **2014**, *258*, 420–423.
[73] S. Y. Hong, Y. Kim, Y. Park, A. Choi, N.-S. Choi, K. T. Lee, *Energy Environ. Sci.* **2013**, *6*, 2067–2081.
[74] T. Yamanaka, A. Hayashi, A. Yamauchi, M. Tatsumisago, *Solid State Ionics* **2014**, *262*, 601–603.
[75] H. D. Yoo, I. Shterenberg, Y. Gofer, G. Gershinsky, N. Pour, D. Aurbach, *Energy Environ. Sci.* **2013**, *6*, 2265–2279.
[76] a) T. Inada, K. Takada, A. Kajiyama, M. Kouguchi, H. Sasaki, S. Kondo, M. Watanabe, M. Murayama, R. Kanno, *Solid State Ionics* **2003**, *158*, 275–280; b) T. Inada, T. Kobayashi, N. Sonoyama, A. Yamada, S. Kondo, M. Nagao, R. Kanno, *J. Power Sources* **2009**, *194*, 1085–1088; c) S. Ito, S. Fujiki, T. Yamada, Y. Aihara, Y. Park, T. Y. Kim, S.-W. Baek, J.-M. Lee, S. Doo, N. Machida, *J. Power Sources* **2014**, *248*, 943–950.
[77] G. Zhou, F. Li, H.-M. Cheng, *Energy Environ. Sci.* **2014**, *7*, 1307–1338.

Received: July 20, 2014
Accepted: November 14, 2014
Published online: ■■ ▮▮, 0000

Israel Journal of Chemistry

REVIEWS

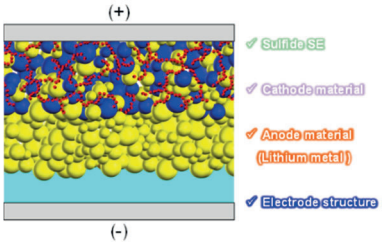

Y. S. Jung, D. Y. Oh, Y. J. Nam, K. H. Park*

■■–■■

Issues and Challenges for Bulk-Type All-Solid-State Rechargeable Lithium Batteries using Sulfide Solid Electrolytes